

Spatially Periodic Orbits in Coupled Sine Circle Maps

Nandini Chatterjee^{1*} and Neelima Gupte^{2 †}

¹ Department of Physics,
University of Pune,
Pune 411007, INDIA.

² Department of Physics,
Indian Institute of Technology, Madras
Madras 600036, INDIA.

We study spatially periodic orbits for a coupled map lattice of sine circle maps with nearest neighbour coupling and periodic boundary conditions. The stability analysis for an arbitrary spatial period k is carried out in terms of the independent variables of the problem and the stability matrix is reduced to a neat block diagonal form. For a lattice of size kN , we show that the largest eigenvalue for the stability matrix of size $kN \times kN$ is the same as that for the basic spatial period k matrix of size $k \times k$. Thus the analysis for a kN lattice case can be reduced to that for a k lattice case. We illustrate this explicitly for a spatial period two case. Our formalism is general and can be extended to any coupled map lattice. We also obtain the stability regions of solutions which have the same spatial and temporal period numerically. Our analysis shows that such regions form a set of Arnold tongues in the $\Omega - \epsilon - K$ space. The tongues corresponding to higher spatial periods are contained within the tongues seen in the temporally periodic spatial period one or synchronised case. We find an interesting new bifurcation wherein the the spatially synchronised and temporal period one solution undergoes a bifurcation to a spatio-temporal period two travelling wave solution. The edges of the stability interval of this solution are analytically obtained.

PACS number(s) : 05.45. +b

arXiv:chao-dyn/9702015v1 23 Feb 1997

*Electronic Mail : nandini@imsc.ernet.in

†Electronic Mail : gupte@imsc.ernet.in

It is well known that systems with many degrees of freedom show complex spatio-temporal behaviour [1]. This behaviour may lead to highly structured self-organising patterns, or may be highly incoherent in the spatial or temporal sense. Studies of systems like Josephson-Junction lattice arrays [2,3], multi-mode lasers [4], reaction-diffusion equations [5], charge density waves [6] and biological systems [7,8] have provided evidence of the rich variety of behaviour that appears in such extended systems. The analysis of such systems via nonlinear partial differential equations has proved to be extremely difficult. On the other hand, the modelling of spatially extended systems by coupled, dynamically evolving elements situated at the discrete sites of a lattice has turned out to be analytically and computationally tractable and has yet succeeded in capturing phenomena like spatio-temporal intermittency [9], pattern formation [10], phase separation [11–13] and chemical wave propagation processes [5,14] which occur in realistic systems.

A striking feature of the spatially extended systems described above, is the existence of regimes where the systems show highly structured and spatially coherent behaviour. Spatially periodic behaviour has been seen in coupled oscillator arrays [15,16], charge density waves [17], biological systems [8,18] and many others. There has been much recent interest in the study of the simplest spatially periodic mode, that of synchronized behaviour in a variety of systems like coupled oscillator arrays [19–21], coupled pendulums [22], electronic oscillator circuits [23], and in pattern formation [24]. Systems of coupled sine circle maps [25] appear to encapsulate some of the generic behaviour found in such systems. Studies of spatially periodic behaviour in coupled sine circle map lattices may yield some insight into the spatially periodic behaviour seen in such systems.

We study the stability of spatially periodic behaviour in a one dimensional system of coupled sine circle maps with nearest neighbour diffusive coupling and periodic boundary conditions. The problem is recast in terms of convenient sum and difference variables which reduce the stability matrix to a neat block diagonal form. We set up the problem for a lattice of size kN , where k is the basic spatial period and N is the number of copies of this basic spatial period that can be contained in the lattice. The stability matrix in this case has size $kN \times kN$. We reduce this matrix to a block diagonal form of N blocks each of size $k \times k$. Further, we obtain the general form for these $k \times k$ matrices, and use the Gerschgorin theorem to show that the largest eigenvalue of the $kN \times kN$ matrix is the same as that of the $k \times k$ matrix corresponding to the basic spatial period. Thus the stability analysis for a lattice of size kN is reduced to that for a lattice of size k .

We carry out the numerical stability analysis of spatially periodic solutions. In particular we find numerically the regions of stability in parameter space of spatially periodic solutions whose temporal period is the same as their spatial period. We find that such solutions form a set of Arnold tongues in the three parameter $\Omega - \epsilon - K$ space of the coupled sine circle map system. Solutions corresponding to higher spatial periods are contained within the tongues seen in the temporally periodic spatial period one or synchronised case [25]. We also obtain a Devil's staircase for such solutions at $K = 1$. An interesting observation from the Arnold tongue plot is the existence of a new bifurcation within the largest tongue, wherein the the spatially synchronised and temporal period one solution undergoes a bifurcation to a spatio-temporal period two travelling wave solution. The stability analysis of the travelling wave solution can be very conveniently carried out in terms of the new variables and the edges of the stability interval of this solution are analytically obtained.

The paper is organized as follows. In section I we consider a lattice of sine circle maps with nearest neighbour diffusive coupling and periodic boundary conditions for a lattice of kN sites which can support a basic spatial period k which is replicated N times. (See Fig.1a ($k = 2$ and $N = 3$) for an illustration of this). We first analyse the linear version or the coupled shift map case and obtain the largest eigen value of the stability matrix for a solution with spatial period k , and then set up the stability matrix for the full nonlinear version. We identify the independent variables for any arbitrary spatial period k , and carry out a linear stability analysis for such a solution for any arbitrary temporal behaviour in terms of these independent variables. In section II, we carry out similarity transformations using direct products of Fourier matrices which reduce a $kN \times kN$ stability matrix to N blocks each of size $k \times k$. Further reduction of the eigen-value analysis of N matrices of size $k \times k$ to that of a single matrix of size $k \times k$, is achieved in section II.A. We demonstrate that the largest eigenvalue for a spatial period k solution in a lattice of kN sites is the same as the largest eigenvalue for a spatial period k solution in a lattice of k sites. As a result, it is sufficient to look at the eigenvalues of the basic spatial period i.e. the $k \times k$ matrix instead of a $kN \times kN$ matrix to obtain the stability conditions for a spatial period k solution. An explicit demonstration for a spatial period two case which is special is carried out in section II.B. Section III discusses numerical simulations for various spatiotemporally periodic solutions. We obtain the regions of stability of various spatiotemporal solutions with the same spatial and temporal period in the $\Omega - \epsilon - K$ space. We obtain interesting plots which resemble the Arnold tongues seen for the spatially synchronized and temporally periodic solution [25] of the $\Omega - \epsilon - K$ space. These tongues are contained within the tongues obtained for the spatially synchronized solution and also display the symmetry about $\Omega = \frac{1}{2}$. We obtain the Devil's staircase for $K = 1$ in the $\Omega - \epsilon - \frac{P}{Q}$ space and discuss its features. We obtain an interesting new bifurcation in the temporal period one tongue ($\Omega = 0$ and $\Omega = 1$) which gives rise to a spatial period two, temporal period two solution which is of the travelling wave type. In section IV we discuss the travelling wave solution. We

carry out a linear stability analysis for the travelling wave solution in terms of the independent variables defined earlier which turn out to be convenient for this analysis. We then obtain analytically the edge for the ϵ interval for such a travelling wave solution with spatial period two and temporal period two at $\Omega = 0$ and $K = 1$. We conclude with section V which discusses results and applications to various physical situations.

I. THE MODEL AND FORMULATION

The specific model under study, is a 1-dimensional coupled map lattice of sine-circle maps with nearest neighbour diffusive symmetric normalized coupling (also called future coupled laplacian coupling) and periodic boundary conditions [25,26]. This is defined by the evolution equation

$$\begin{aligned} \theta_{t+1}(i) = & (1 - \epsilon) \left(\theta_t(i) + \Omega - \frac{K}{(2\pi)} \sin(2\pi\theta_t(i)) \right) \\ & + \frac{\epsilon}{2} \left\{ \theta_t(i+1) + \Omega - \frac{K}{(2\pi)} \sin(2\pi\theta_t(i+1)) \right. \\ & \left. + \theta_t(i-1) + \Omega - \frac{K}{(2\pi)} \sin(2\pi\theta_t(i-1)) \right\} \quad \text{mod } 1 \end{aligned} \quad (1)$$

where $\theta_t(i)$ is the angular variable associated with the i th lattice site, at time t and lies between 0 and 1, K is the strength of the nonlinearity, Ω is the period of the system for $K = 0$ and ϵ which lies between 0 and 1 is the strength of the coupling parameter. We study the system for the homogeneous parameter case where Ω and K take the same value at each lattice site. However the framework we develop can be used to study inhomogenous systems where the values of Ω and K depend on the lattice site.

We consider a lattice of kN sites and are interested in periodic solutions such that k is the basic spatial period and N is the number of copies of this basic spatial period. For example, in Fig.1(a), we have a lattice of six lattice sites for which alternate lattice sites have the same value. Hence it is a spatial period two solution and $k = 2$. This basic block is repeated three times so we have $N = 3$. In this paper we show how the stability analysis for a lattice of kN sites can be reduced to just the study of the basic period of the k lattice site case. We show that to study the stability properties of a spatial period two solution in a lattice of six sites, instead of looking at the eigen-value of the full 6×6 dimensional stability matrix it is sufficient to look at the largest eigenvalue arising out of the period two solution of a lattice of two sites i.e. the eigenvalue of a matrix of size 2×2 .

A. The shift map case

We begin with the simplest case which is $K = 0$, i.e. the coupled shift map case. This is just the linear version of the circle map and is a much simpler system to study than the full non-linear version [25].

We consider a system of kN coupled shift maps with nearest neighbour diffusive symmetric coupling and periodic boundary conditions. As illustrated in Fig.1(a) (where $k = 2$ and $N = 3$), this is a lattice which can support a solution with basic spatial period k and N replica solutions. The evolution equations are

$$\theta_{t+1}(i) = (1 - \epsilon) \left(\theta_t(i) + \Omega \right) + \frac{\epsilon}{2} \left(\theta_t(i+1) + \theta_t(i-1) \right) + \epsilon\Omega \quad \text{mod } 1 \quad (2)$$

We observe that for a spatial period k solution, at any time t , the value of the variable at the i th lattice site is the same as the value at the $(i+k)$ th site. Thus, the difference between the variable values of the i th and the $(i+k)$ th lattice site, approaches zero for all such pairs of neighbours.

Setting up the evolution equation for such a difference we have

$$\begin{aligned} \theta_{t+1}(i) - \theta_{t+1}(i+k) = & (1 - \epsilon) \left(\theta_t(i) - \theta_t(i+k) \right) \\ & + \frac{\epsilon}{2} \left(\theta_t(i+1) - \theta_t(i+k+1) + \theta_t(i-1) - \theta_t(i+k-1) \right) \end{aligned} \quad (3)$$

Eq. 3 can be completely expressed in terms of the differences $a_t^k(i)$ defined as

$$a_t^k(i) = \theta_t(i) - \theta_t(i+k) \quad (4)$$

where the superscript k denotes the spatial period at any time t .

The differences thus evolve as

$$a_{t+1}^k(i) = (1 - \epsilon)(a_t^k(i)) + \frac{\epsilon}{2} \left(a_t^k(i+1) + a_t^k(i-1) \right) \quad \text{mod } 1 \quad (5)$$

It can be easily seen that $a_t^k(i) = 0$, is a spatial period k solution for Eq.5.

Expanding upto the linear term about this solution leads to a stability matrix J_t^{kN} [27] given by

$$J_t^{kN} = \begin{pmatrix} (1 - \epsilon) & \frac{\epsilon}{2} & 0 & 0 & \cdots & 0 & 0 & \frac{\epsilon}{2} \\ \frac{\epsilon}{2} & (1 - \epsilon) & \frac{\epsilon}{2} & 0 & 0 & \cdots & 0 & 0 \\ 0 & \frac{\epsilon}{2} & (1 - \epsilon) & \frac{\epsilon}{2} & 0 & \cdots & 0 & 0 \\ \vdots & \vdots \\ \frac{\epsilon}{2} & 0 & 0 & \cdots & 0 & 0 & \frac{\epsilon}{2} & (1 - \epsilon) \end{pmatrix} \quad (6)$$

This is a $kN \times kN$ matrix, which is also circulant and whose eigen values maybe explicitly obtained analytically. The eigenvalues of J_t^{kN} are given by [25,29]

$$\lambda_r = (1 - \epsilon) + \frac{\epsilon}{2}(\omega_r + \omega_r^{-1}) \quad (7)$$

where ω_r is the kN th root of unity given by

$$\omega_r = \exp\left(\frac{2i\pi(r-1)}{kN}\right) \quad (8)$$

On simplifying, this can be written as

$$\lambda_r = (1 - \epsilon) + \epsilon \cos\left(\frac{2\pi(r-1)}{kN}\right) \quad r = 1, 2, \dots, kN \quad (9)$$

The stability condition for spatially periodic (with period k) orbits of the coupled shift map is given by $\lambda^{largest} \leq 1$, the largest eigenvalue of Eq. 9. It can be easily seen that the largest eigen value is $+1$, indicating that the coupled shift map is marginally stable. This is true for all spatial periods k , including the spatially synchronised case, $k = 1$ [25]. Thus if we start off with initial conditions that correspond to a spatially periodic solution, we remain on them. The temporal period depends on the value of Ω and we obtain temporally periodic orbits of period Q for rational values of $\Omega = P/Q$ and quasiperiodic orbits for irrational values of Ω .

B. The coupled circle map case

A similar analysis can be carried out for a lattice of sine circle maps of kN sites as defined in Eq. 1. We look for the regions of stability of spatially periodic solutions with spatial period k for a lattice of kN sites.

As in the coupled shift map case, here too we observe that at time t for a fixed Ω and K and a particular spatial period k the difference between the i th and $(i+k)$ th lattice sites is zero. (Fig. 1a). The difference is again defined as

$$a_t^k(i) = \theta_t(i) - \theta_t(i+k) \quad (10)$$

Using Eq.1 and setting up the equation of evolution for the differences it can be easily seen that the evolution equation for these differences involves not just terms which involve the differences $a_t^k(i)$ but also terms of the kind $(\theta_t(i) + \theta_t(i+k))$ which is just the sum of the variables of the i th and $i+k$ th site. We also observe that at a fixed Ω and K and spatial period k that the sum of the i th and $i+k$ th site is also a constant. So we now define

$$b_t^k(i) = \theta_t(i) + \theta_t(i+k) \quad (11)$$

$$\forall i; 1, \dots, kN$$

Using Eq.1 we obtain the equations of evolution for $a_t^k(i)$ and $b_t^k(i)$ as

$$\begin{aligned}
a_{t+1}^k(i) &= (1 - \epsilon) \left(a_t^k(i) - \frac{K}{\pi} \sin(\pi a_t^k(i)) \cos(\pi b_t^k(i)) \right) \\
&+ \frac{\epsilon}{2} \left(a_t^k(i+1) - \frac{K}{\pi} \sin(\pi a_t^k(i+1)) \cos(\pi b_t^k(i+1)) \right) \\
&+ \frac{\epsilon}{2} \left(a_t^k(i-1) - \frac{K}{\pi} \sin(\pi a_t^k(i-1)) \cos(\pi b_t^k(i-1)) \right) \quad \text{mod } 1
\end{aligned} \tag{12}$$

and

$$\begin{aligned}
b_{t+1}^k(i) &= (1 - \epsilon) \left(b_t(i) - \frac{K}{\pi} \sin(\pi b_t^k(i)) \cos(\pi a_t^k(i)) \right) \\
&+ \frac{\epsilon}{2} \left(b_t^k(i+1) - \frac{K}{\pi} \sin(\pi b_t^k(i+1)) \cos(\pi a_t^k(i+1)) \right) \\
&+ \frac{\epsilon}{2} \left(b_t^k(i-1) - \frac{K}{\pi} \sin(\pi b_t^k(i-1)) \cos(\pi a_t^k(i-1)) \right) + 2\Omega \quad \text{mod } 1
\end{aligned} \tag{13}$$

It can be easily shown that, $\forall i$, $a_t^k(i) = 0$ and $b_t^k(i) = s_m$ ($m \equiv i \pmod{k}$), where s_1, s_2, \dots, s_k are all distinct *constants*, are solutions of Eq.12 and 13 for a fixed Ω and K .

To study the stability of any spatially periodic solution with spatial period k we need to examine the eigenvalues of the linear stability matrix. We expand Eqs. 12 and 13 about $a_t^k(i) = 0$ and $b_t^k(i) = s_m, m : 1, 2 \dots k$ distinct constants, upto the linear order and obtain the matrix of coefficients J_t^{2kN} . (Since we have two sets of equations namely for the $a_t^k(i)$'s and $b_t^k(i)$'s each for kN sites, the dimension of the matrix J_t^{2kN} is $2kN \times 2kN$). The largest eigenvalue of this matrix crossing 1 determines the edge of stability for the corresponding spatiotemporal solution. We have

$$J_t^{2kN} = \begin{pmatrix} A_t'^{kN} & B_t'^{kN} \\ B_t'^{kN} & A_t'^{kN} \end{pmatrix} \tag{14}$$

where

$$A_t'^{kN} = \begin{pmatrix} \epsilon_s A_t^k(1) & \epsilon_n A_t^k(2) & 0 & \cdots & 0 & \epsilon_n A_t^k(kN) \\ \epsilon_n A_t^k(1) & \epsilon_s A_t^k(2) & \epsilon_n A_t^k(3) & 0 & \cdots & 0 \\ 0 & \epsilon_n A_t^k(2) & \epsilon_s A_t^k(3) & \cdots & 0 & 0 \\ \vdots & \vdots & \vdots & \vdots & \vdots & \vdots \\ \epsilon_n A_t^k(1) & 0 & \cdots & 0 & \epsilon_n A_t^k(kN-1) & \epsilon_s A_t^k(kN) \end{pmatrix} \tag{15}$$

and

$$B_t'^{kN} = \begin{pmatrix} \epsilon_s B_t^k(1) & \epsilon_n B_t^k(2) & 0 & \cdots & 0 & \epsilon_n B_t^k(kN) \\ \epsilon_n B_t^k(1) & \epsilon_s B_t^k(2) & \epsilon_n B_t^k(3) & 0 & \cdots & 0 \\ 0 & \epsilon_n B_t^k(2) & \epsilon_s B_t^k(3) & \cdots & 0 & 0 \\ \vdots & \vdots & \vdots & \vdots & \vdots & \vdots \\ \epsilon_n B_t^k(1) & 0 & \cdots & 0 & \epsilon_n B_t^k(kN-1) & \epsilon_s B_t^k(kN) \end{pmatrix} \tag{16}$$

where ϵ_s, ϵ_n are given by

$$\epsilon_s = (1 - \epsilon), \quad \epsilon_n = \frac{\epsilon}{2} \tag{17}$$

Here, each

$$A_t^k(i) = \left(1 - K \cos(\pi a_t^k(i)) \cos(\pi b_t^k(i)) \right) \tag{18}$$

and

$$B_t^k(i) = \left(K \sin(\pi a_t^k(i)) \sin(\pi b_t^k(i)) \right) \tag{19}$$

where $b_t^k(i)$ repeats after k sites.

Imposing the conditions $a_t^k(i) = 0$ and $b_t^k(i) = s_m$ where $m : 1, 2 \dots k$, the stability matrix J_t^{2kN} given by Eq.14 reduces to a block diagonal form

$$J_t^{2kN} = \begin{pmatrix} M_t^{kN} & 0 \\ 0 & M_t^{kN} \end{pmatrix} \quad (20)$$

where the blocks M_t^{kN} are identical and each M_t^{kN} is of the form,

$$M_t^{kN} = \begin{pmatrix} \epsilon_s \bar{A}_t^k(1) & \epsilon_n \bar{A}_t^k(2) & 0 & \dots & 0 & \epsilon_n \bar{A}_t^k(k) \\ \epsilon_n \bar{A}_t^k(1) & \epsilon_s \bar{A}_t^k(2) & \epsilon_n \bar{A}_t^k(3) & 0 & \dots & 0 \\ 0 & \epsilon_n \bar{A}_t^k(2) & \epsilon_s \bar{A}_t^k(3) & \epsilon_n \bar{A}_t^k(4) & 0 & \dots \\ \vdots & \vdots & \vdots & \vdots & \vdots & \vdots \\ \epsilon_n \bar{A}_t^k(1) & 0 & \dots & 0 & \epsilon_n \bar{A}_t^k(k-1) & \epsilon_s \bar{A}_t^k(k) \end{pmatrix} \quad (21)$$

and each

$$\bar{A}_t^k(i) = \left(1 - K \cos(\pi s_i)\right) \quad (22)$$

where, each m goes from $1, \dots, k$ and repeats after k sites and $m \equiv imodk$. We thus obtain the stability matrix in a block diagonal form as given by Eq. 20 where each M_t^{kN} is a matrix of size $kN \times kN$. We now carry out matrix transformations which reduce the matrix M_t^{kN} which is a $kN \times kN$ matrix into a block diagonal form with N matrices each of size $k \times k$. Thus a $kN \times kN$ matrix is reduced to N matrices each of size $k \times k$. Further we use Gerschgorin's theorem for eigen values of square matrices which reduces the stability analysis of the problem from the analysis of N matrices of size $k \times k$ to that of just one matrix of size $k \times k$ - the basic spatial period k matrix.

II. REDUCTION OF THE STABILITY MATRIX

We now illustrate the reduction of the matrix M_t^{kN} for a spatial period $k > 2$. The spatial period corresponding to $k = 1$ is the synchronized solution where M_t^{kN} turns out to be a circulant matrix and has been discussed in Ref. [25]. The case $k = 2$ has special features which will be discussed in a separate section below. We consider the matrix M_t^{kN} of Eq. 21 where $k > 2$. Using a similarity transformation we now reduce the matrix M_t^{kN} which has dimensions $kN \times kN$ into a block diagonal matrix of N blocks each of size $k \times k$. The similarity transformation which achieves this, is a direct product of Fourier matrices of size $N \times N$ and $k \times k$.

A Fourier matrix F_k (where k denotes the dimension of the matrix) is defined as

$$F_k^*(i, j) = \frac{1}{\sqrt{k}} (\omega_k^{(i-1)(j-1)}) \quad (23)$$

F_k is easily calculated as the conjugate transpose of F_k^* and $\omega_k = e^{\frac{2\pi i}{k}}$.

The similarity transformation for a stability matrix of size $kN \times kN$, which achieves the block diagonal form is given by

$$F_{kN} = F_N \otimes F_k \quad (24)$$

where \otimes indicates direct product.

For example, for a six lattice site case and a spatial period two solution, we have $k = 2$ and $N = 3$, i.e we have three replicas of the spatial period two solution. Constructing Fourier matrices F_2 and F_3 we obtain,

$$F_2^* = \frac{1}{\sqrt{2}} \begin{pmatrix} 1 & 1 \\ 1 & -1 \end{pmatrix} \quad (25)$$

and

$$F_3^* = \frac{1}{\sqrt{3}} \begin{pmatrix} 1 & 1 & 1 \\ 1 & \frac{-1+i\sqrt{3}}{2} & \frac{-1-i\sqrt{3}}{2} \\ 1 & \frac{-1-i\sqrt{3}}{2} & \frac{-1+i\sqrt{3}}{2} \end{pmatrix} \quad (26)$$

A direct product of F_3 and F_2 will give us a 6×6 matrix which is required for the similarity transformation for a lattice of 6 sites where the basic spatial period (k) is 2 and the number of copies (N) is 3. Since Fourier matrices are also unitary the conjugate transpose of this matrix is also its inverse and so F_k^* is the inverse of F_k .

The operation $F_{kN} M_t^k F_{kN}^*$ gives the following block diagonal form for M_t^{kN}

$$M_t^{kN} = \begin{pmatrix} M_t^k(1) & 0 & 0 & \cdots & 0 \\ 0 & M_t^k(2) & 0 & 0 & \cdots \\ \vdots & \vdots & \vdots & \vdots & \vdots \\ 0 & 0 & 0 & M_t^k(l-1) & 0 \\ 0 & 0 & 0 & 0 & M_t^k(l) \end{pmatrix} \quad (27)$$

where l goes from $1, 2 \dots N$.

For $k > 2$, each $M_t^k(l)$ is a $k \times k$ matrix and has a structure of the form

$$M_t^k(l) = \begin{pmatrix} \epsilon_s \bar{A}_t^k(1) & \epsilon_n \bar{A}_t^k(2) & 0 & \cdots & 0 & \epsilon_n \bar{A}_t^k(k) \omega_l \\ \epsilon_n \bar{A}_t^k(1) & \epsilon_s \bar{A}_t^k(2) & \epsilon_n \bar{A}_t^k(3) & 0 & \cdots & 0 \\ 0 & \epsilon_n \bar{A}_t^k(2) & \epsilon_s \bar{A}_t^k(3) & \epsilon_n \bar{A}_t^k(4) & 0 & \cdots \\ \vdots & \vdots & \vdots & \vdots & \vdots & \vdots \\ \epsilon_n \bar{A}_t^k(1) \omega_l^{-1} & 0 & \cdots & 0 & \epsilon_n \bar{A}_t^k(k-1) & \epsilon_s \bar{A}_t^k(k) \end{pmatrix} \quad (28)$$

where ω_l is defined as $\omega_l = e^{\frac{2\pi i}{k}}$ and $\bar{A}_t^k(i)$ is as defined in Eq.22. A similar block diagonal form will be achieved for the $k = 2$ case as well but the matrix $M_t^k(l)$ has a different form for $k = 2$ which will be discussed later.

A. Reduction to the basic spatial period - the $k \times k$ case $k > 2$

We now use Gerschgorin's theorem [28] for square matrices which states that the eigen values of a matrix A_m (of dimension m) lie in the union of all points Λ such that

$$|\Lambda - a_{ii}| \leq C_i, i = 1, 2 \dots m \quad (29)$$

where

$$C_i = \sum_j' |a_{ij}| \quad (30)$$

where \sum_j' indicates that the summation is for $j = 1, 2 \dots, m$ excluding $j = i$ and a_{ij} is the ij th element of the matrix A_m .

By this theorem if one constructs circles in the complex plane for $i = 1, 2 \dots m$ with the elements a_{ii} as centres and the sum of the absolute values of the remaining elements in the i th row as the corresponding radii, then each eigen value of A_m must lie in or on one of the circles, the Gerschgorin discs [28].

We now consider a lattice of k sites and the stability of a spatial period k solution. We have only one block for a lattice of k sites, and a spatial period k solution, so $l = 1$ in Eq. 27 and $M_t^k(l)$ is given by

$$M_t^k(1) = \begin{pmatrix} (1 - \epsilon)c_1 & \frac{\epsilon}{2}c_2 & 0 & \cdots & 0 & \frac{\epsilon}{2}c_k \\ \frac{\epsilon}{2}c_1 & (1 - \epsilon)c_2 & \frac{\epsilon}{2}c_3 & 0 & \cdots & 0 \\ 0 & \frac{\epsilon}{2}c_2 & (1 - \epsilon)c_3 & \frac{\epsilon}{2}c_4 & 0 & \cdots \\ \vdots & \vdots & \vdots & \vdots & \vdots & \vdots \\ \frac{\epsilon}{2}c_1 & 0 & \cdots & 0 & \frac{\epsilon}{2}c_{k-1} & (1 - \epsilon)c_k \end{pmatrix} \quad (31)$$

where $c_i = (1 - K \cos(\pi b_t^k(i)))$ and $\omega_l = 1$.

The Gerschgorin discs for this matrix will be k circles of the following form.

$$(x - (1 - \epsilon)c_i)^2 + y^2 = \left(\left| \frac{\epsilon}{2}c_{i+1} \right| + \left| \frac{\epsilon}{2}c_{i-1} \right| \right)^2 \quad (32)$$

where $i = 1 \dots k$.

Thus according to Gerschgorin's theorem all the characteristic or eigen values of this matrix will lie in or on these circles.

For a lattice of size kN , we now construct circles for the matrix $M_t^k(l)$ given by Eq. 28. The general form of matrix $M_t^k(l)$ (Eq. 28) differs from that in Eq. 31 in the form of the first row and the last row. So while considering the eigen values of $M_t^k(l)$ we need to construct Gerschgorin discs only for the first row and the last row, the remaining $k-2$ Gerschgorin discs will be the same as those obtained for the k lattice case above. For the $M_t^k(l)$ matrix we have the following equation for the first Gerschgorin disc

$$\begin{aligned} (x_1 - (1 - \epsilon)c_1)^2 + y_1^2 &= \left(\left| \frac{\epsilon}{2}c_2 \right| + \left| \frac{\epsilon}{2}c_k\omega_l \right| \right)^2 \\ &= \left(\left| \frac{\epsilon}{2}c_2 \right| + \left| \frac{\epsilon}{2}c_k \right| |\omega_l| \right)^2 \end{aligned} \quad (33)$$

Similarly the equation of the k th Gerschgorin disc is given by

$$\begin{aligned} (x_k - (1 - \epsilon)c_k)^2 + y_k^2 &= \left(\left| \frac{\epsilon}{2}c_{k-1} \right| + \left| \frac{\epsilon}{2}c_1\omega_l^{-1} \right| \right)^2 \\ &= \left(\left| \frac{\epsilon}{2}c_{k-1} \right| + \left| \frac{\epsilon}{2}c_1 \right| |\omega_l^{-1}| \right)^2 \end{aligned} \quad (34)$$

ω_l is defined as $\omega_l = e^{\frac{2\pi i}{k}}$. Hence $|\omega_l|$ and $|\omega_l^{l-1}|$ is 1. Thus Eqs.33 and 34 reduce to

$$(x_1 - (1 - \epsilon)c_1)^2 + y_1^2 = \left(\left| \frac{\epsilon}{2}c_2 \right| + \left| \frac{\epsilon}{2}c_k \right| \right)^2 \quad (35)$$

and

$$(x_k - (1 - \epsilon)c_k)^2 + y_k^2 = \left(\left| \frac{\epsilon}{2}c_{k-1} \right| + \left| \frac{\epsilon}{2}c_1 \right| \right)^2 \quad (36)$$

So all the eigen values of the matrix $M_t^k(l)$ will lie in or on one of these circles. Thus the eigen values of all the N matrices (as $l : 1, 2 \dots N$) will lie in or on one of these Gerschgorin circles.

But these are precisely the Gerschgorin discs we obtained for the matrix M_t^k i.e. the matrix for a lattice of k sites and spatial period k as obtained Eq. 32.

The stability of any spatially periodic solution is obtained by checking where the largest eigenvalue crosses the unit circle, with $\lambda^{largest} = \pm 1$ being the condition for marginal stability. The analysis presented above shows that the bounds on the eigenvalues for the $kN \times kN$ matrix given by Eqs. 32, 35 and 36 for the kN lattice case are the same as the bounds on the eigenvalues for the $k \times k$ matrix given by Eqs. 32 i.e. that of the k lattice case which is also the basic spatial period. Thus the largest eigenvalue for $M_t^k(1)$ crosses 1 for the same parameter values as the largest eigenvalue of $M_t^k(l)$ ($l : 1, \dots N$) crosses 1. We thus conclude that it is sufficient to check for the largest eigenvalue of the basic $k \times k$ matrix as given by Eq.32 to decide the stability properties for any multiple of k too namely kN . The bounds on the eigenvalue for a spatial period k solution for a lattice of k sites will remain the same for a spatial period k solution and a lattice of kN sites. We now illustrate this explicitly for a spatial period 2 case and thus a $2N$ case.

B. The $k = 2$ case - Illustration for a $2N$ site lattice

Consider the spatial period two case for two lattice sites which evolve via the evolution equations 12 and 13. (See Fig.1(a)).

Here $\theta_t(i+2)$ is the same as $\theta_t(i)$

The stability matrix for a spatial period two solution is given by

$$M_t^2(1) = \begin{pmatrix} (1 - \epsilon)c_1 & \epsilon c_2 \\ \epsilon c_1 & (1 - \epsilon)c_2 \end{pmatrix} \quad (37)$$

Here

$$\begin{aligned} c_1 &= (1 - K \cos(\pi s_1)) \\ c_2 &= (1 - K \cos(\pi s_2)) \end{aligned}$$

It is clear from Eq. 37 that the stability matrix for a spatial period $k = 2$, two lattice site case is not of the same form as that for $k > 2$. Since each of the two sites has just one neighbour, each site is coupled to its neighbour with a coupling constant of strength ϵ , and is coupled to itself with strength $1 - \epsilon$, in contrast with the $k > 2$ case where each site has two neighbours and is coupled to each of its neighbours with a coupling constant of strength $\frac{\epsilon}{2}$ and to itself with strength $1 - \epsilon$. The overall normalisation of the coupling is preserved in both cases. This results in the general form of the matrix $M_t^{2N}(l)$ having a different form for the $k = 2$ case as compared to the general k case, $k > 2$ (Eq. 28).

Since M_t^2 is a 2×2 matrix the eigenvalues may be easily obtained and are given by

$$\lambda = \frac{(1 - \epsilon)(c_1 + c_2)}{2} \pm \frac{1}{2} \sqrt{(1 - \epsilon)^2(c_1 + c_2)^2 - 4(1 - 2\epsilon)c_1c_2} \quad (38)$$

It can be easily shown that the eigenvalue corresponding to the $+$ sign is the larger one.

Now consider a lattice of $2N$ sites where N is any positive integer. We carry out the above analysis for a spatial period two solution and obtain the matrix $M_t^2(l)$ where $l : 1 \dots N$. Any $M_t^2(l)$ is of the form

$$M_t^2(l) = \begin{pmatrix} (1 - \epsilon)c_1 & \frac{\epsilon}{2}(1 + \omega_l)c_2 \\ \frac{\epsilon}{2}(1 + \omega_l^{-1})c_1 & (1 - \epsilon)c_2 \end{pmatrix} \quad (39)$$

where c_1 and c_2 are as defined above and ω_l is the N th root of unity and depends on the number of replicas. For $N = 3$ i.e. six lattice sites, $l : 1, \dots, 3$ (in this case $k = 2$). $M_t^2(l)$ has a different form for the $k = 2$ case as mentioned above.

The eigen-values of the $2N$ case turn out to be

$$\lambda = \frac{(1 - \epsilon)(c_1 + c_2)}{2} \pm \frac{1}{2} \sqrt{(1 - \epsilon)^2(c_1 + c_2)^2 - 4c_1c_2(1 - \epsilon)^2 + c_1c_2\epsilon^2(2 + 2\cos(2\pi\frac{l-1}{2}))} \quad (40)$$

The largest eigen value is obtained for $\cos(\frac{2\pi(l-1)}{2}) = 1$ (which occurs for $l = 1, 3, 5 \dots$). The largest eigenvalue is

$$\lambda = \frac{(1 - \epsilon)(c_1 + c_2)}{2} + \frac{1}{2} \sqrt{(1 - \epsilon)^2(c_1 + c_2)^2 - 4(1 - 2\epsilon)c_1c_2} \quad (41)$$

Comparing the largest eigenvalue of Eq. 38 and that of Eq. 41 we find that the largest eigen value obtained for the $2N$ lattice case is the same as that obtained for the 2 lattice case. Thus for a $2N$ lattice it is sufficient to look at the stability properties for just two lattice sites which is the basic k period. ($k = 2$ in this case).

Gerschgorin's theorem may also be used to prove the above. Using Gerschgorin's theorem for the matrix defined by Eq. 37 we find that all the eigen values of this matrix will lie in or on the circles given by the equations

$$\begin{aligned} (x_1 - (1 - \epsilon)c_1)^2 + y_1^2 &= (\epsilon c_2)^2 \\ (x_2 - (1 - \epsilon)c_2)^2 + y_2^2 &= (\epsilon c_1)^2 \end{aligned} \quad (42)$$

Constructing Gerschgorin discs again, now for Eq. 39 we have the following circles.

$$\begin{aligned} (x_1 - (1 - \epsilon)c_1)^2 + y_1^2 &= \left| \frac{\epsilon}{2} c_2 (1 + \omega_l) \right|^2 \\ (x_2 - (1 - \epsilon)c_2)^2 + y_2^2 &= \left| \frac{\epsilon}{2} c_1 (1 + \omega_l^{-1}) \right|^2 \end{aligned} \quad (43)$$

where ω_l is defined as $\omega_l = e^{\frac{2\pi i}{N}}$ and $l : 1, 2 \dots N$.

Using the definition of ω_l Eq. 43 reduces to

$$\begin{aligned} (x_1 - (1 - \epsilon)c_1)^2 + y_1^2 &= (\epsilon c_2)^2 \cos^2\left(\frac{\pi}{N}\right) \\ (x_2 - (1 - \epsilon)c_2)^2 + y_2^2 &= (\epsilon c_1)^2 \cos^2\left(\frac{\pi}{N}\right) \end{aligned} \quad (44)$$

The radii on the r.h.s. of Eq. 44 have a maximum value for $l = 1$ for which the equations of the Gerschgorin circles obtained are the same as those obtained in Eqs. 42. But $l = 1$ is just the basic $k = 2$ period (two lattice site case). Thus the bounds on the largest eigenvalue obtained for a spatial period two solution for a lattice of $2N$ sites are the same as that obtained for the spatial period two solution for a two lattice site case and it is sufficient to look at the stability matrix of the basic spatial period ($k = 2$) case for the eigen-value analysis.

III. NUMERICAL ANALYSIS

We carry out the numerical stability analysis for spatiotemporal solutions with the same spatiotemporal period i.e solutions of the kind spatial period 3 and corresponding temporal period 3 and spatial period 2 and temporal period 2 and so on. Analysis is carried out in terms of the new variables namely $a_t^k(i)$ and $b_t^k(i)$.

We define the following vector notation,

$$\vec{f}_a(\vec{a}, \vec{b}, \vec{\Omega}) \rightarrow \{f_{1a}(\vec{a}, \vec{b}, \vec{\Omega}), f_{2a}(\vec{a}, \vec{b}, \vec{\Omega}), \dots, f_{Na}(\vec{a}, \vec{b}, \vec{\Omega})\} \quad (45)$$

where $\vec{f}_a(\vec{a}, \vec{b}, \vec{\Omega})$ denotes the evolution of $a_t^k(i)$ as given by Eq.12. and

$$\vec{f}_b(\vec{a}, \vec{b}, \vec{\Omega}) \rightarrow \{f_{1b}(\vec{a}, \vec{b}, \vec{\Omega}), f_{2b}(\vec{a}, \vec{b}, \vec{\Omega}), \dots, f_{Nb}(\vec{a}, \vec{b}, \vec{\Omega})\} \quad (46)$$

where $\vec{f}_b(\vec{a}, \vec{b}, \vec{\Omega})$ denotes the evolution of $b_t^k(i)$ given by Eq.13.

For a lattice of kN sites, each i denotes the lattice index and each component of \vec{a} and \vec{b} is defined by Eqs.12 and 13 respectively. Each a and b is now a vector of the form

$$\begin{aligned} (\vec{a}) &\rightarrow \{a_t^k(1), a_t^k(2), \dots, a_t^k(kN)\} \\ (\vec{b}) &\rightarrow \{b_t^k(1), b_t^k(2), \dots, b_t^k(kN)\} \end{aligned} \quad (47)$$

and the parameter, Ω , also a vector, is represented as

$$(\vec{\Omega}) \rightarrow \{\Omega(1), \Omega(2), \dots, \Omega(N)\} \rightarrow \{\Omega, \Omega, \dots, \Omega\} \quad (48)$$

The Ω 's, could have different values at different sites, but in this case have the same value at each site. For a 1-d array of coupled sine circle maps, the stability criterion is obtained by examining the eigen values of the corresponding stability matrix. From Eq.20 we obtain the fact that the two blocks in the linear stability matrix, the M_t^k are identical. We consider one of these in the analysis and for the calculation of the eigenvalues. After simplification we obtain a $k \times k$ matrix corresponding to the k th spatial period and temporal period Q given by

$$S_Q^k = \prod_{t=1}^Q \begin{pmatrix} \frac{\partial f_{1a}}{\partial a_t^k(1)} & \frac{\partial f_{1a}}{\partial a_t^k(2)} & \dots & \frac{\partial f_{1a}}{\partial a_t^k(k)} \\ \frac{\partial f_{2a}}{\partial a_t^k(1)} & \frac{\partial f_{2a}}{\partial a_t^k(2)} & \dots & \frac{\partial f_{2a}}{\partial a_t^k(k)} \\ \vdots & \vdots & \ddots & \vdots \\ \frac{\partial f_{ka}}{\partial a_t^k(1)} & \frac{\partial f_{ka}}{\partial a_t^k(2)} & \dots & \frac{\partial f_{ka}}{\partial a_t^k(k)} \end{pmatrix} \quad (49)$$

The second M_t^k which is obtained is identical and is obtained by calculating the entries $\frac{\partial f_{mb}}{\partial b_t^k(j)}$ where $m : 1, 2 \dots k$ and for each $m, j : 1, 2 \dots k$.

We consider any one of these matrices and then obtain the eigenvalues of the simplified M_t^k .

Let $\{\lambda_i\}$ be the set of eigenvalues of the matrix S_t . For a period Q orbit to be stable the eigenvalues of the matrix $S_Q^k < 1$. The largest eigenvalue crossing 1 defines the marginal stability condition.

Thus for the higher order temporal periods, we seek the solution to the following set of equations

$$\begin{aligned} \vec{f}^Q(\vec{a}, \vec{b}, \vec{\Omega}) &= (\vec{a}) + \vec{P} \\ \vec{f}^Q(\vec{a}, \vec{b}, \vec{\Omega}) &= (\vec{b}) + \vec{P} \end{aligned} \quad (50)$$

as the conditions of closure, namely the differences $a_t^k(t)$ and the sums $b_t^k(i)$. Since we are looking for spatiotemporally periodic solutions we check for spatial closure too in the following way.

$$\begin{aligned} \vec{f}_a(i+k) &= \vec{f}_a(i) \\ \vec{f}_b(i+k) &= \vec{f}_b(i) \end{aligned} \quad (51)$$

The condition for marginal stability is given by

$$\lambda^{largest} = 1 \quad (52)$$

We start with initial conditions corresponding to the particular spatiotemporal period under study and obtain points in the $\Omega - \epsilon - K$ phase space where the given spatiotemporal solution is closed and is stable. We find the stability edges in the $\epsilon - \Omega$ plane for each value of K using bisection method upto an accuracy of 10^{-8} .

A. The $\Omega - \epsilon - K$ plot

We plot the regions of stability in the $\Omega - \epsilon - K$ phase space for spatial periods $k = 2, 3, 4$. We confine our search to regions of stability for solutions which have the same spatial and temporal period. The stability regions for such solutions form a set of Arnold tongues in the $\Omega - \epsilon - K$ space (See Fig.3). Similar tongues were seen earlier for the $k = 1$ or synchronised solution for different temporal periods [25]. The tongues for higher spatial periods are contained within the Arnold tongues of the spatially synchronized and temporally periodic solution of the same temporal period. The tongues are symmetric about $\Omega = 0.5$ as in the case of the single circle map and the synchronised solution of the coupled sine circle map lattice.

The study of two dimensional slices in the $\Omega - \epsilon$ space for a fixed value of K show that the ϵ tongue develops a finite width for values of K lower than those at which the Ω tongue develops a finite width (See Fig.4(a)-(c)). Fig. 4(a) reveals that for a small value of $K = 0.016$, the ϵ tongue shows a width while there is no width in Ω yet. Figs.4(b) and 4(c) show slices at $K = 0.14$ and $K = 0.15$ respectively illustrating the opening of the $\Omega = \frac{1}{2}$ tongue. Figs.4(b) and 4(c) also show that when the $\Omega = \frac{1}{2}$ tongue opens, a finite width of ϵ at $\Omega = 0.495$ and $\Omega = 0.505$ is seen. We thus conclude that since the ϵ width is observed for a lower value of $K (= 0.015)$ than the Ω width ($K = 0.15$) spatial orbits stabilize faster than temporal orbits.

An interesting new bifurcation is seen in the $\Omega = \frac{0}{1}$ and $\frac{1}{1}$ tongue. Starting with spatial period two initial conditions, one would expect spatial period one, temporal period one or spatial period two temporal period one solutions within this tongue [25]. Instead, the tongue now also contains travelling wave solutions with spatiotemporal period two. They show widths in the Ω and ϵ space which widen with increasing K and arise as a result of a spatiotemporal bifurcation of the spatially synchronized and temporal period one solution. We discuss these solutions in detail in a separate section where we also obtain the stability interval of the ϵ region for $\Omega = 0$ and $K = 1$ analytically.

The tongues in the $\Omega - \epsilon - K$ phase plane are confined to $\epsilon < 0.5$ i.e. we obtain stable closed spatiotemporal solutions for $\epsilon < 0.5$. We thus conclude that lower values of ϵ or smaller couplings lead to stable solutions where the spatial and temporal periods are equal. However, the $K = 0$ or the coupled shift map case shows marginally stable orbits at rational values of Ω for all values of ϵ .

B. The $\Omega - \epsilon - \frac{P}{Q}$ plot

We plot the stable regions for solutions with temporal winding number $\frac{P}{Q}$ in the $\Omega - \epsilon$ space at $K = 1$ for spatial periods $k = Q$ in Fig.4(a). We thus obtain the widths of various spatiotemporal solutions, $\frac{P}{Q} = \frac{1}{2}, \frac{1}{3}, \frac{2}{3}, \frac{1}{4}, \frac{3}{4}, \frac{1}{5}, \frac{2}{5}, \frac{3}{5}, \frac{4}{5}$ in the $\Omega - \epsilon$ space at $K = 1$. This forms a series of steps of finite $\Omega - \epsilon$ width for the observed values of $\frac{P}{Q}$. This is similar to the Devil's staircase seen in the case of the single circle map and the synchronised solution [25,26]. However the width of the step for each $\frac{P}{Q}$ is no longer independent of ϵ as it was for the synchronized case but depends on ϵ . The staircase is symmetric about $\Omega = 0.5$. Fig. 6 shows a two dimensional plot of the $\Omega - \epsilon$ space at $K = 1$ for various values of the winding number $\frac{P}{Q}$. The travelling wave solution shows the largest width in ϵ at $\Omega = 0$ which decreases as Ω increases.

IV. THE TRAVELLING WAVE SOLUTION

We now discuss the travelling wave solution seen in the $\Omega = 0$ and $\Omega = 1$ tongues. Starting with spatial period two initial conditions in the $\Omega = 0$ and $\Omega = 1$ tongues we expect to find spatial period one or spatial period two solutions with a temporal fixed point solution. However we find a spatial period two solution which also has temporal period two in the $\Omega = 0$ and $\Omega = 1$ tongue which has the travelling wave structure as seen in Fig. 1(b). This is the new bifurcation we obtain in the $\Omega = 0$ and $\Omega = 1$ tongues. Starting with spatial period two initial conditions we find after a certain critical value of ϵ , travelling wave solutions of the period two kind are obtained in the $\Omega = 0$ and $\Omega = 1$ tongue. We analytically show that stable travelling wave solutions appear after a critical value of ϵ and obtain the width of the ϵ tongue for $\Omega = 0$ and $K = 1$. The independent variables of the problem, namely the differences and the sums turn out to be convenient variables for this analysis.

Since we find a bifurcation from a spatially synchronised temporal period one solution to a spatial period two temporal period two solution of the travelling wave type we consider a lattice of $2N$ sites and construct nearest neighbour differences and sums defined as

$$\begin{aligned}
\tilde{a}_t(i) &= \theta_t(i) - \theta_t(i+1) \\
\tilde{b}_t(i) &= \theta_t(i) + \theta_t(i+1)
\end{aligned} \tag{53}$$

The evolution eqns. for $\tilde{a}_t(i)$ and $\tilde{b}_t(i)$ are given by Eqs. 12 and 13 (with $k = 1$).

$$\begin{aligned}
\tilde{a}_{t+1}(i) &= (1 - \epsilon) \left(\tilde{a}_t(i) - \frac{K}{\pi} \sin(\pi \tilde{a}_t(i)) \cos(\pi \tilde{b}_t(i)) \right) \\
&\quad + \frac{\epsilon}{2} \left(\tilde{a}_t(i+1) - \frac{K}{\pi} \sin(\pi \tilde{a}_t(i+1)) \cos(\pi \tilde{b}_t(i+1)) \right) \\
&\quad + \frac{\epsilon}{2} \left(\tilde{a}_t(i-1) - \frac{K}{\pi} \sin(\pi \tilde{a}_t(i-1)) \cos(\pi \tilde{b}_t(i-1)) \right) \pmod{1}
\end{aligned} \tag{54}$$

and

$$\begin{aligned}
\tilde{b}_{t+1}(i) &= (1 - \epsilon) \left(\tilde{b}_t(i) - \frac{K}{\pi} \sin(\pi \tilde{b}_t(i)) \cos(\pi \tilde{a}_t(i)) \right) \\
&\quad + \frac{\epsilon}{2} \left(\tilde{b}_t(i+1) - \frac{K}{\pi} \sin(\pi \tilde{b}_t(i+1)) \cos(\pi \tilde{a}_t(i+1)) \right) \\
&\quad + \frac{\epsilon}{2} \left(\tilde{b}_t(i-1) - \frac{K}{\pi} \sin(\pi \tilde{b}_t(i-1)) \cos(\pi \tilde{a}_t(i-1)) \right) + 2\Omega \pmod{1}
\end{aligned} \tag{55}$$

Consider Fig. 1(b) which shows the travelling wave solution for which the spatial and temporal period is two. This solution can be expressed in a very compact form in terms of the sum and difference variables. The differences $\tilde{a}_t(i)$'s are equal but no longer zero as in the synchronized case. Again, the sums $\tilde{b}_t(i)$'s are equal to some constant as in the synchronized case, but in addition it is clear that $\tilde{b}_{t+1}(i) = \tilde{b}_t(i)$ reflecting the travelling wave nature of the solution. Thus,

$$\begin{aligned}
\tilde{a}_t(i) &= -\tilde{a}_t(i+1) \neq 0 \\
\tilde{a}_{t+1}(i) &= \tilde{a}_t(i+1) = -\tilde{a}_t(i)
\end{aligned} \tag{56}$$

and

$$\begin{aligned}
\tilde{b}_t(i) &= \tilde{b}_t(i+1) \\
\tilde{b}_{t+1}(i) &= \tilde{b}_t(i) = \text{constant}
\end{aligned} \tag{57}$$

The two conditions above are specific to the spatiotemporal period two solution of the travelling wave type. Similar equations can be set up in general for travelling wave solutions of spatiotemporal period k .

We use evolution equations for $\tilde{a}_t(i)$ and $\tilde{b}_t(i)$ and carry out a linear stability analysis about the travelling wave solutions which are expressed in terms of Eqs. 56 and 57. We obtain the stability matrix by expanding about the solutions $\tilde{a}_t = \text{constant}$ and $\tilde{b}_t = \text{constant}$. The linear stability matrix is given by

$$J_t^{4N} = \begin{pmatrix} \tilde{A}_t^{2N} & \tilde{B}_t^{2N} \\ \tilde{B}_t^{2N} & \tilde{A}_t^{2N} \end{pmatrix} \tag{58}$$

where \tilde{A}_t^{2N} and \tilde{B}_t^{2N} are $2N \times 2N$ matrices which are given by

$$\tilde{A}_t^{2N} = \begin{pmatrix} \epsilon_s \tilde{A}_t(1) & \epsilon_n \tilde{A}_t(2) & 0 & \cdots & 0 & \epsilon_n \tilde{A}_t(2) \\ \epsilon_n \tilde{A}_t(1) & \epsilon_s \tilde{A}_t(2) & \epsilon_n \tilde{A}_t(1) & 0 & \cdots & 0 \\ 0 & \epsilon_n \tilde{A}_t(2) & \epsilon_s \tilde{A}_t(1) & \epsilon_n \tilde{A}_t(2) & 0 & \cdots \\ \vdots & \vdots & \vdots & \vdots & \vdots & \vdots \\ \epsilon_n \tilde{A}_t(1) & 0 & \cdots & 0 & \epsilon_n \tilde{A}_t(1) & \epsilon_s \tilde{A}_t(2) \end{pmatrix} \tag{59}$$

and

$$\tilde{B}_t^{2N} = \begin{pmatrix} \epsilon_s \tilde{B}_t(1) & \epsilon_n \tilde{B}_t(2) & 0 & \cdots & 0 & \epsilon_n \tilde{B}_t(2) \\ \epsilon_n \tilde{B}_t(1) & \epsilon_s \tilde{B}_t(2) & \epsilon_n \tilde{B}_t(1) & 0 & \cdots & 0 \\ 0 & \epsilon_n \tilde{B}_t(2) & \epsilon_s \tilde{B}_t(1) & \epsilon_n \tilde{B}_t(2) & 0 & \cdots \\ \vdots & \vdots & \vdots & \vdots & \vdots & \vdots \\ \epsilon_n \tilde{B}_t(1) & 0 & \cdots & 0 & \epsilon_n \tilde{B}_t(1) & \epsilon_s \tilde{B}_t(2) \end{pmatrix} \quad (60)$$

where ϵ_s, ϵ_n are given by Eq.17

Here, each

$$\tilde{A}_t(i) = \left(1 - K \cos(\pi \tilde{a}_t(i)) \cos(\pi \tilde{b}_t(i))\right) \quad (61)$$

and

$$\tilde{B}_t(i) = K \sin(\pi \tilde{a}_t(i)) \sin(\pi \tilde{b}_t(i)) \quad (62)$$

Using the conditions $\tilde{b}_t(1) = \tilde{b}_t(2)$ and $\tilde{a}_t(1) = -\tilde{a}_t(2)$ (seen from definition of the differences and Fig.1b) \tilde{A}'_t and \tilde{B}'_t reduce to matrices given by

$$\tilde{A}'_t^{2N} = \begin{pmatrix} \epsilon_s \tilde{A}'_t(1) & \epsilon_n \tilde{A}'_t(1) & 0 & \cdots & 0 & \epsilon_n \tilde{A}'_t(1) \\ \epsilon_n \tilde{A}'_t(1) & \epsilon_s \tilde{A}'_t(1) & \epsilon_n \tilde{A}'_t(1) & 0 & \cdots & 0 \\ 0 & \epsilon_n \tilde{A}'_t(1) & \epsilon_s \tilde{A}'_t(1) & \epsilon_n \tilde{A}'_t(1) & 0 & \cdots \\ \vdots & \vdots & \vdots & \vdots & \vdots & \vdots \\ \epsilon_n \tilde{A}'_t(1) & 0 & \cdots & 0 & \epsilon_n \tilde{A}'_t(1) & \epsilon_s \tilde{A}'_t(1) \end{pmatrix} \quad (63)$$

and

$$\tilde{B}'_t^{2N} = \begin{pmatrix} \epsilon_s \tilde{B}'_t(1) & -\epsilon_n \tilde{B}'_t(1) & 0 & \cdots & 0 & -\epsilon_n \tilde{B}'_t(1) \\ \epsilon_n \tilde{B}'_t(1) & -\epsilon_s \tilde{B}'_t(1) & \epsilon_n \tilde{B}'_t(1) & 0 & \cdots & 0 \\ 0 & -\epsilon_n \tilde{B}'_t(1) & \epsilon_s \tilde{B}'_t(1) & -\epsilon_n \tilde{B}'_t(1) & 0 & \cdots \\ \vdots & \vdots & \vdots & \vdots & \vdots & \vdots \\ \epsilon_n \tilde{B}'_t(1) & 0 & \cdots & 0 & \epsilon_n \tilde{B}'_t(1) & -\epsilon_s \tilde{B}'_t(1) \end{pmatrix} \quad (64)$$

and each

$$\tilde{A}'_t(i) = \left(1 - K \cos \pi \tilde{a}_t(1) \cos \pi \tilde{b}_t(1)\right) \quad (65)$$

$$\tilde{B}'_t(i) = K \sin \pi \tilde{a}_t(1) \sin \pi \tilde{b}_t(1) \quad (66)$$

Using simple matrix algebra, J_t^{4N} can be put into a block diagonal form given by

$$J_t^{4N} = \begin{pmatrix} M_t^{2N}(+) & 0 \\ 0 & M_t^{2N}(-) \end{pmatrix} \quad (67)$$

where

$$\begin{aligned} M_t^{2N}(+) &= \tilde{A}'_t^{2N} + \tilde{B}'_t^{2N} \\ M_t^{2N}(-) &= \tilde{A}'_t^{2N} - \tilde{B}'_t^{2N} \end{aligned} \quad (68)$$

The matrices $M_t^{2N}(+)$ and $M_t^{2N}(-)$ are similar ($M_t^{2N}(-) = \pi M_t^{2N}(+) \pi$, where π is the permutation matrix) and thus have the same characteristic polynomial and it is sufficient to consider the eigenvalues of one of them.

Following the treatment outlined in Section II B for a lattice of $2N$, we use a similarity transformation which is a direct product of Fourier matrices of size $N \times N$ and 2×2 which reduces $M_t^{2N}(+)$ to a matrix of N blocks, each block of size 2×2 . For the travelling wave solution of spatial and temporal period two $M_t^2(l)$ is given by

$$M_t^2(l) = \begin{pmatrix} (1 - \epsilon)(\tilde{A}'_t(1) + \tilde{B}'_t(1)) & \frac{\epsilon}{2}(1 + \omega_l)(\tilde{A}'_t(1) - \tilde{B}'_t(1)) \\ \frac{\epsilon}{2}(1 + \omega_l^{-1})(\tilde{A}'_t(1) + \tilde{B}'_t(1)) & (1 - \epsilon)(\tilde{A}'_t(1) - \tilde{B}'_t(1)) \end{pmatrix} \quad (69)$$

where ω_l is as defined before and $l : 1, 2 \dots N$. As also discussed in Section II B, this can be reduced to the analysis of just two lattice sites and $M_t^2(1)$ is given by

$$M_t^2(1) = \begin{pmatrix} (1 - \epsilon)(\tilde{A}'_t(1) + \tilde{B}'_t(1)) & \epsilon(\tilde{A}'_t(1) - \tilde{B}'_t(1)) \\ \epsilon(\tilde{A}'_t(1) + \tilde{B}'_t(1)) & (1 - \epsilon)(\tilde{A}'_t(1) - \tilde{B}'_t(1)) \end{pmatrix} \quad (70)$$

The eigenvalues of this matrix are given by

$$\lambda = (1 - \epsilon)\tilde{A}'_t(1) \pm \sqrt{\epsilon^2\tilde{A}'_t(1)^2 + (1 - 2\epsilon)\tilde{B}'_t(1)^2} \quad (71)$$

The largest eigenvalue $\tilde{\lambda}$ is the one corresponding to the + sign and is given by

$$\tilde{\lambda} = (1 - \epsilon)(1 - K \cos \pi \tilde{a}_t(1) \cos \pi \tilde{b}_t(1)) + \sqrt{\epsilon^2(1 - K \cos \pi \tilde{a}_t(1) \cos \pi \tilde{b}_t(1))^2 + (1 - 2\epsilon)(K \sin \pi \tilde{a}_t(1) \sin \pi \tilde{b}_t(1))^2} \quad (72)$$

Using the condition for closure and the largest eigenvalue we can obtain the widths of the ϵ interval for which stable travelling wave solutions are obtained.

A. Illustration for the $\Omega = 0$ case

For $\Omega = 0$ and $K = 1$, substituting the travelling wave conditions given by Eqs. 56 and 57 in the evolution equation for $\tilde{b}_t(i)$ namely Eqs. 54 and 55 we obtain

$$\frac{1}{\pi} \sin \pi \tilde{b}_t(1) \cos \pi \tilde{a}_t(1) = 0 \quad (73)$$

which implies

$$\tilde{b}_t(1) = 0, 1, 2, \dots n \quad (74)$$

or

$$\tilde{a}_t(1) = \frac{1}{2}, \frac{3}{2}, \dots \frac{2n+1}{2} \quad (75)$$

If we consider Eq. 72 we observe that if $\tilde{a}_t(1)$ is $\frac{1}{2} \pmod{1}$ and $\tilde{b}_t(1)$ arbitrary, the eigenvalue is > 1 and thus unstable. Hence for stable travelling wave solutions at $\Omega = 0$ and $K = 1$ we consider Eq. 74.

Using Eq. 74 in Eq. 54, the evolution equation for $\tilde{a}_t(i)$ we get,

$$(1 - \epsilon)\tilde{a}_t(1) + \frac{(1 - 2\epsilon)}{2\pi} \sin(\pi\tilde{a}_t(1)) = 0 \quad (76)$$

We consider the case where $\tilde{b}_t(1) = 1$ and $\tilde{a}_t(1)$ is arbitrary, a condition also observed in numerical simulations. The case $b_t = 0$ corresponds to the smaller eigenvalue and $b_t = 2$ and above are ruled out due to the fact that $\theta_t(i)$ always lies between 0 and 1. Thus using $\tilde{b}_t(1) = 1$ and $\tilde{a}_t(1)$ arbitrary, in Eq. 72, the largest eigenvalue is given by

$$\tilde{\lambda} = 1 + \cos(\pi\tilde{a}_t(1)) \quad (77)$$

For the edge of the stable solution, we have

$$1 + \cos(\pi\tilde{a}_t(1)) = 1 \quad (78)$$

which gives

$$\tilde{a}_t(1) = \frac{1}{2}, \frac{3}{2}, \dots \frac{2n+1}{2} \quad (79)$$

which is also what we obtained in Eq. 75.

Thus for a stable spatiotemporal period two travelling wave solution, the edge is obtained for $\tilde{a}_t(1) = 0.5 \pmod{1}$. Using $\tilde{a}_t(1) = 0.5$ in Eq. 76 we obtain $\epsilon = \frac{(\pi+1)}{(2+\pi)}$ which gives $\epsilon = 0.805523$. We have also obtained these solutions numerically and Fig. 6 shows the travelling wave bifurcation along with other spatiotemporally periodic solutions. Fig. 6 is a two dimensional plot of the widths in ϵ for various values of $\frac{L}{Q}$ at $K = 1$. Comparing the value obtained numerically for the lower edge of the interval for $\Omega = 0$ and $K = 1$ we obtain a close agreement with computational accuracy. The travelling wave solution is discontinuous at $\epsilon = 1$ as at this value we obtain $\tilde{a}_t(i) = 0$ which is a synchronised solution and is thus no longer a travelling wave solution.

Similarly the evolution equations for $\tilde{a}_t(i)$ and $\tilde{b}_t(i)$ alongwith Eqs. 54,55 and 72 can be solved for fixed Ω and K to obtain the corresponding width in ϵ .

V. CONCLUSIONS AND DISCUSSION

We have studied the stability of spatially periodic solutions in a lattice of coupled sine circle maps. The stability analysis of a system of kN lattice sites with N copies of the basic spatial period k has been reduced to the analysis of $N = 1$ copies of the basic spatial period k by an appropriate choice of variables, a similarity transformation via Fourier matrices and the use of the Gerschgorin theorem. We have provided an explicit illustration of this for a spatial period 2 case and a $2N$ site lattice. Our analysis is completely general and can be applied to other coupled map lattice systems as well.

We have also studied stability of solutions where the spatial and temporal periods are equal, and found their regions of stability in the $K - \epsilon - \Omega$ space numerically. We find that the stability regions of such solutions show an Arnold tongue structure in the parameter space. We also see a Devil's staircase of winding numbers at $K = 1$ in the $\Omega - \epsilon - \frac{P}{Q}$ space. A new and interesting feature observed in the case of the $\frac{0}{1}$ and $\frac{1}{1}$ tongues is the existence of a bifurcation to a spatial period two, temporal period two solution of the travelling wave type. The stability edge for this solution can also be obtained analytically. The method can be easily extended to travelling wave solutions in other coupled map lattices.

The framework set up by us should be useful in the analysis of the spatially periodic behaviour seen in a variety of situations like reaction-diffusion equations, coupled laser arrays, biological systems. It should also be interesting to investigate the correspondence between the synchronised to travelling wave bifurcation seen by us and the in-phase to splay phase bifurcation seen in Josephson Junction arrays [2], anti-phase behaviour in multimode lasers [4], or the synchronised to rotating wave behaviour seen in rings of coupled chaotic oscillators [30]. We hope our study will find useful applications in some of these contexts.

ACKNOWLEDGMENTS

We thank the Institute of Mathematical Sciences, Madras, for computing facilities. One of the authors (NC) gratefully acknowledges CSIR (India), for financial support.

References

- [1] J. P. Crutchfield, and K. Kaneko in *Directions in Chaos*, edited by Hao-Bai Lin (World Scientific, Singapore, 1987), **Vol 3** and references therein.
- [2] K. Wiesenfeld and J. W. Swift, Phys. Rev. E **51**, 1020, (1995).
- [3] A. A. Chernikov and G. Schmidt, Phys. Rev. E **52**, 3415 (1995).
- [4] K. Wiesenfeld, C. Bracikowski, G. James, and R. Roy, Phys. Rev. Lett. **64**, 1749 (1990)
- [5] R. Kapral in *Theory and Applications of Coupled Map Lattices*, edited by K. Kaneko (John Wiley, England, 1993) and references therein.
- [6] H. Sompolskiy, D. Golomb, and D. Kleinfeld, Phys. Rev. E **43**, 6990 (1991).
- [7] S. H. Strogatz, C. M. Marcus, R. M. Westervelt, and R. Mirollo, Physica D **36**, 23 (1989).
- [8] C. M. Gray et al, Nature **338**, 334, (1989); R. Eckhorn et al., Biol. Cybernetics **60**, 121 (1988).
- [9] H. Chate and P. Manneville, Phys. Rev. Lett **58**, 112 (1987).
- [10] D. Stanssinopoulos and P. Alstrom, Phys. Rev. A **45**, 675 (1992).
- [11] G. L. Oopo and R. Kapral, Phys. Rev. A **36**, 5826 (1987)
- [12] R. Elders, T Rodgers and R. Desai, Phys. Rev. B **38**, 4725 (1988).
- [13] Y. Oono and S. Puri, Phys. Rev. Lett **58**, 836 (1987)
- [14] R. Kapral, J. Math Chem **6**, 113 (1991).
- [15] M. Y. Choi *et al*, Phys. Rev. E **49** 3825 (1994).
- [16] G. L. Oopo and R. Kapral, Phys. Rev. **A33**, 4219 (1985); R. Kapral and G. L. Oopo, Physica **23D**, 455 (1986).
- [17] S. N. Coppersmith, Phys. Rev. A **36**, 3375 (1987).
- [18] P. Davis, Jap. J. Appl. Phys. Lett. **29**, 1238 (1990).
- [19] I. Waller and R. Kapral, Phys. Rev. **30A** 2047 (1984); R. Kapral, Phys. Rev. **31A**, 3868 (1985).
- [20] K. Wiesenfeld and P. Hadley, Phys. Rev. Lett. **62**, 1335 (1989)
- [21] J. F. Heagy, T. L. Carroll and L. M. Pecora Phys. Rev. E **50**, 1874 (1994) and references therein
- [22] F. F. Abraham, Phys. Rev. E **47**, 1625 (1993).
- [23] P. Ashwin *et al.*, Nonlinearity **3**, 585 (1990).
- [24] K. Kaneko, Physica **34 D**, 1-41 (1989).
- [25] N. Chatterjee and N. Gupte, Phys. Rev. E **3** 4457 (1996), Physica A **224**, 422-432 (1996).
- [26] T. Bohr, P. Bak, M. H. Jensen, Phys. Rev. A **30** 1960 (1984).
- [27] We shall assign the superscript 'd' to all stability matrices J_t^d where d denotes the dimension of the matrix and J_t^d is a $d \times d$ matrix.
- [28] M. Stein, *Introduction to Matrices and Determinants* (Wadsworth Publishing Inc., Belmont, California, 1967)
- [29] P. J. Davis, *Circulant Matrices* (Wiley, New York, 1979).
- [30] M.A. Matias, V. Perez-Munuzuri, M.N. Lorenzo, I.P. Marino and V. Perez-Villar, Phys. Rev. Lett. **78**, 219 (1997).

FIGURE CAPTIONS

- Fig.1 (a) The spatially periodic solution with $k = 2$ and $N = 3$.
 k is the basic spatial period, two in this case, which is repeated $N = 3$ times ($kN = 6$ sites)
- Fig.1 (b) The travelling wave solution with spatial period $k = 2$ and temporal period = 2.
 In this case the number of replicas is $N = 3$.
 It can be seen that $a_t(i) = -a_{t+1}(i) = a_t(i + 1)$, $b_t(i) = b_{t+1}(i) = b_t(i + 1)$
- Fig.2 Illustration of Gerschgorin's theorem for the spatial period two ($k = 2$) and temporal period one case. The eigenvalue is analytically obtained to be 0.174334 and 0.193911. For $\epsilon = 0.1$ and $\Omega = 0$ and at $K = 1$ we obtain the stability matrix for k (2) sites and construct circles with radii 0.214 and 0.1929. in accordance with Eq.42. The eigenvalue has been marked with an X
- Fig.3 Arnold tongues for spatiotemporally periodic solutions in a coupled sine circle map lattice. The tongues have been plotted for winding numbers starting from $\frac{P}{Q} = \frac{0}{1}, \frac{1}{1}, \frac{1}{2}, \frac{1}{3}, \frac{2}{3}$ as a function of Ω and ϵ . We also observe an additional new bifurcation within the tongue at $\Omega = 0$ and $\Omega = 1$. This is a travelling wave solution (dashed lines) with spatial period two and temporal period two and has a structure as shown in Fig.1(b).
- Fig.4 (a) The opening of the ϵ tongue. At $K = 0.016$ we observe a finite width in ϵ at $\Omega = \frac{1}{2} = 0.5$. The ϵ tongue opens before the Ω tongue which implies spatially periodic solutions stabilize faster than temporally periodic solutions.
- Fig.4 (b) $\Omega = \frac{1}{2}$ and $\Omega = \frac{1}{3}$ at $K = 0.14$ which show finite widths in ϵ but still no width in Ω .
- Fig.4 (c) Ω values as in Fig.4 (b), now with a finite width in Ω also for $K = 0.15$.
- Fig.5 The Devil's staircase for spatiotemporally periodic solutions with the same winding number $\frac{P}{Q}$ in a coupled sine circle map lattice. The symmetry about $\Omega = 0.5$ is clearly seen. The widths are calculated for $\Delta\Omega(\frac{P}{Q})$ for $\frac{P}{Q} = \frac{0}{1}, \frac{1}{1}, \frac{1}{2}, \frac{1}{3}, \frac{2}{3}, \frac{1}{4}, \frac{3}{4}, \frac{1}{5}, \frac{2}{5}, \frac{3}{5}, \frac{4}{5}$. We see an additional new width at $\frac{P}{Q} = \frac{0}{1}, \frac{1}{1}$. These are travelling wave solutions (dashed lines) with spatial period two and temporal period two.
- Fig.6 A two dimensional slice of the Devil's staircase for the spatiotemporally periodic solutions with winding numbers as in Fig.5. The shape and size of the steps is now dependent on ϵ and symmetry about $\Omega = 0.5$ is clearly seen.

Figure 1aNC and NG

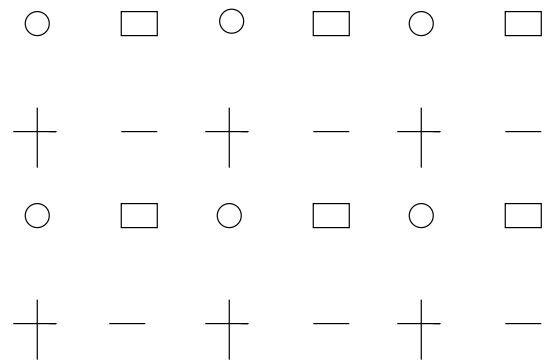


Figure 1bNC and NG

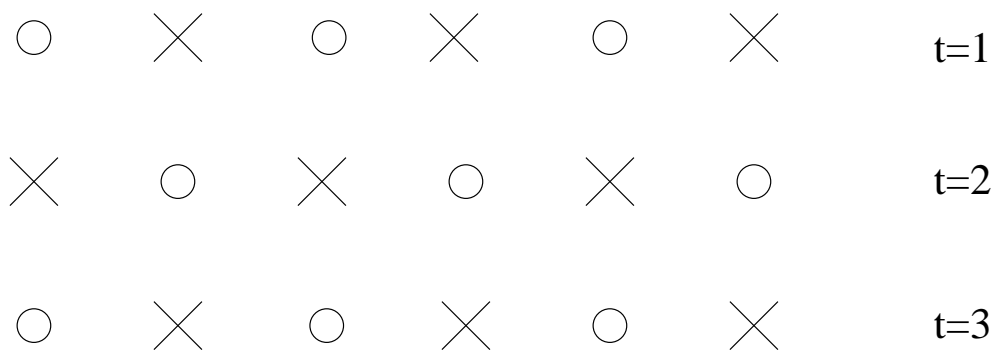


Figure 2 ----- NC and NG

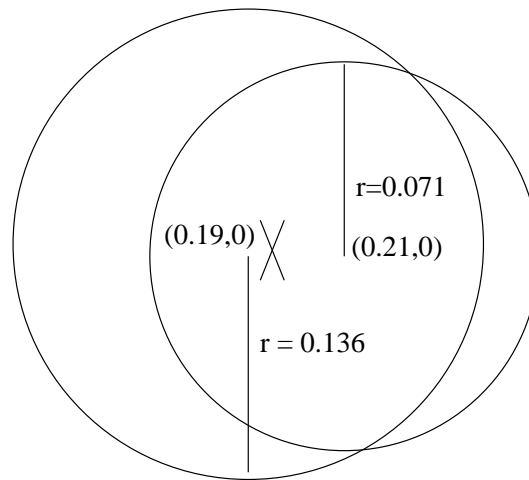


Figure 3 -----NC and NG

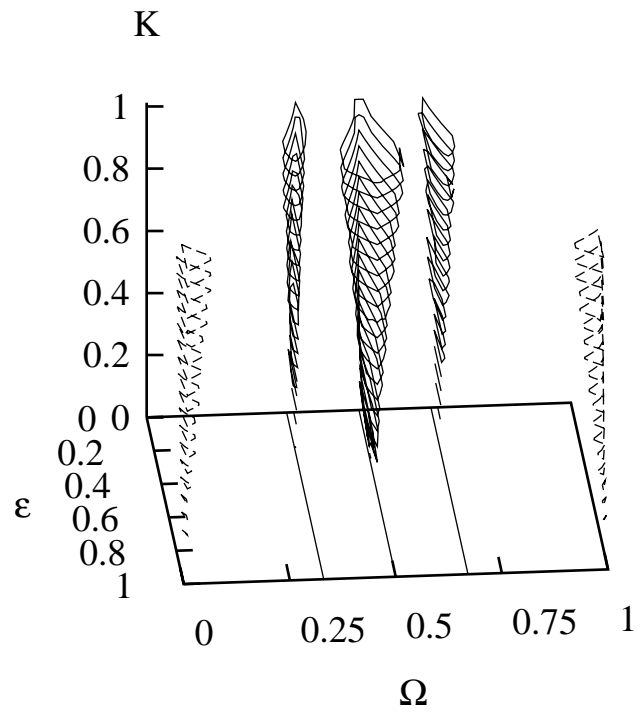


Figure 4 (a)-----NC and NG

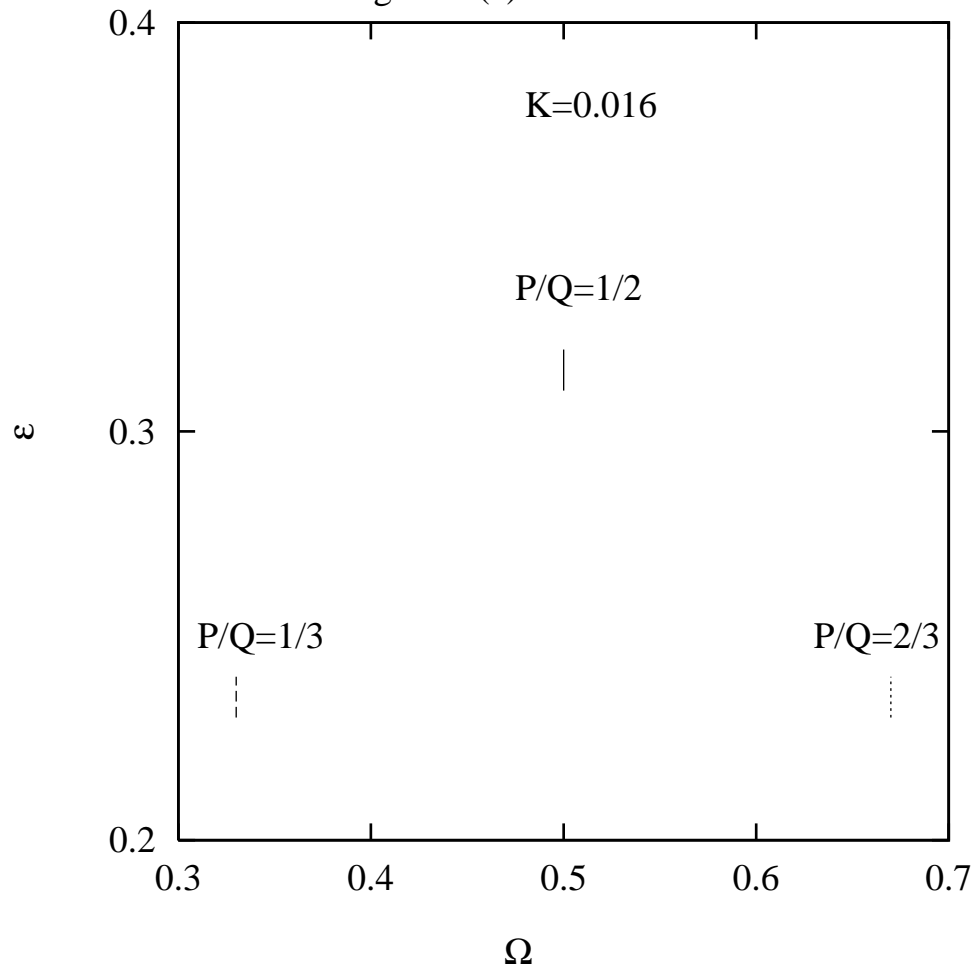


Figure 4 (b)-----NC and NG

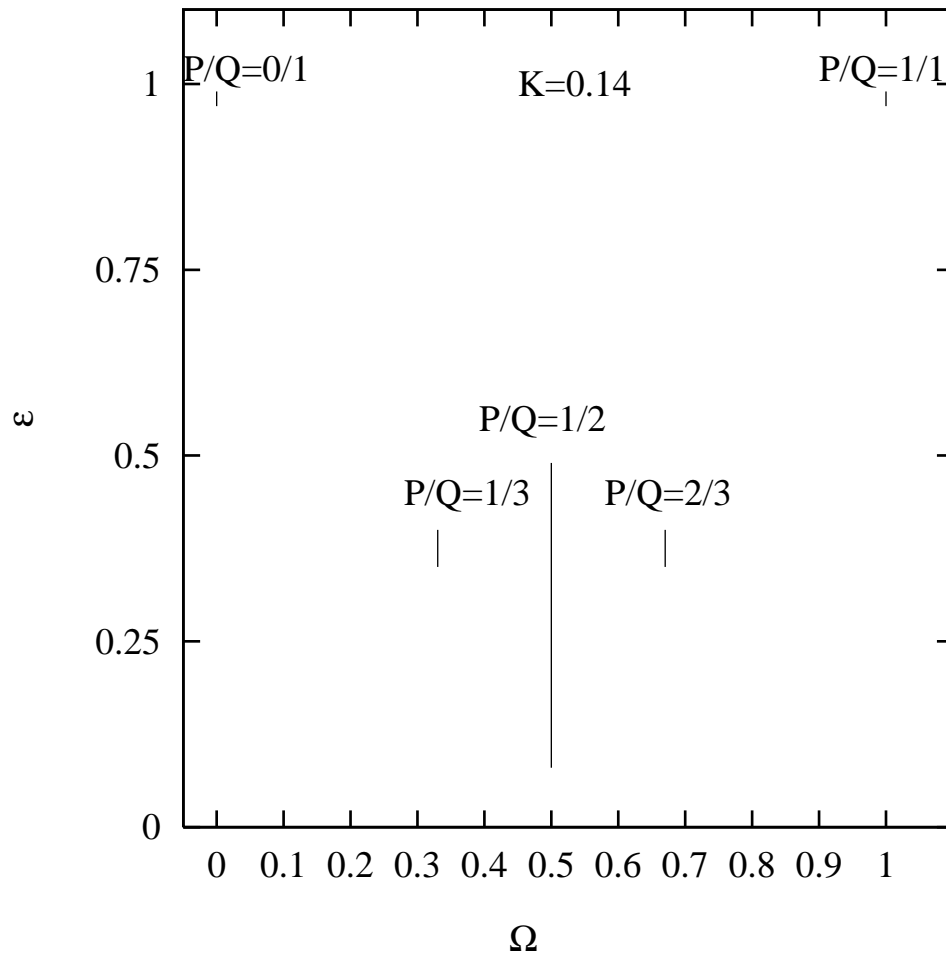


Figure 4 (c)-----NC and NG

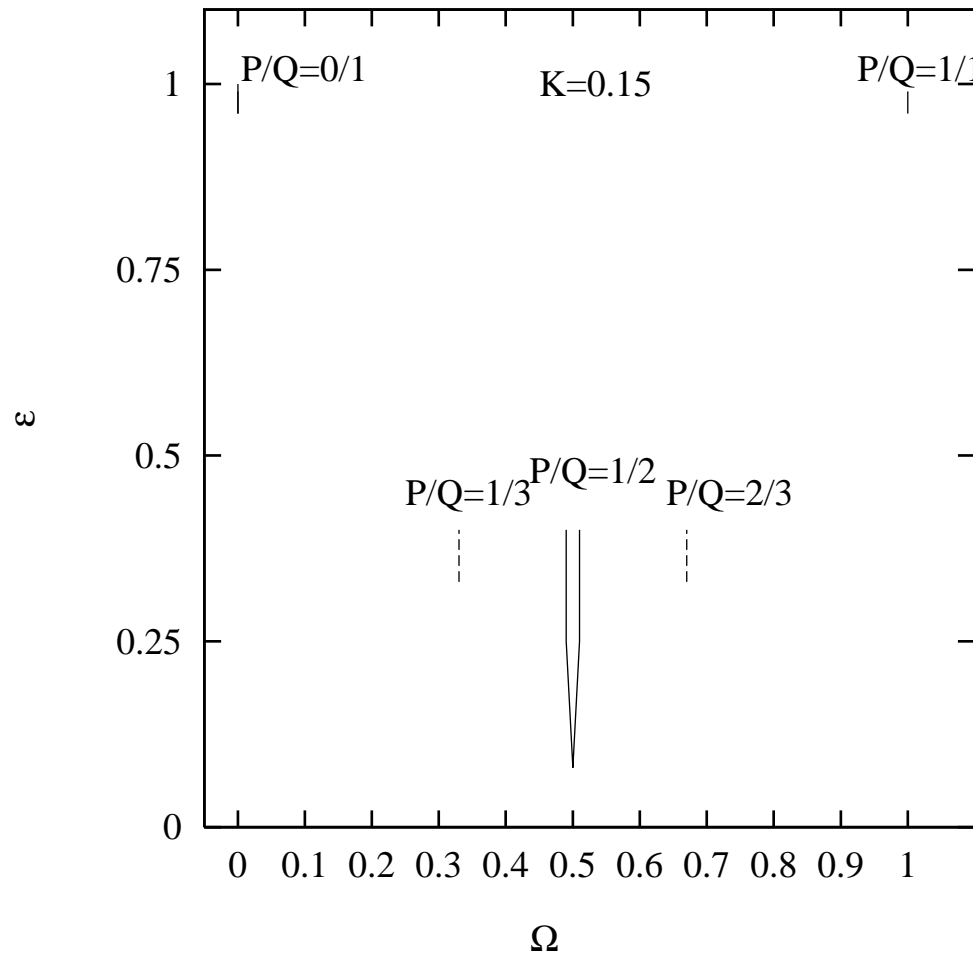


Figure 5 -----NC and NG

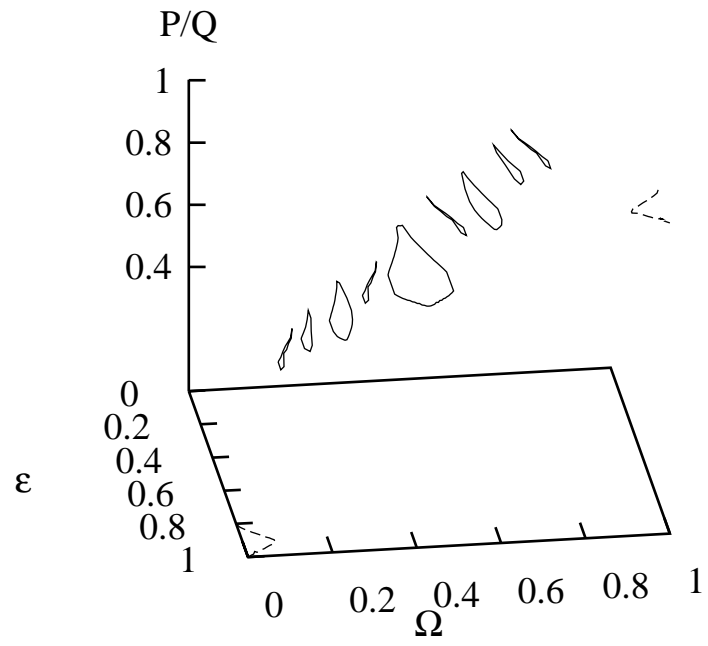


Figure 6 -----NC and NG

